Journal of ELECTRICAL ENGINEERING, VOL. 57, NO. 3, 2006, 146–153

CIR MEASUREMENT SYSTEM FOR CHARACTERISATION OF WIDEBAND COMMUNICATION CHANNELS IN THE 2.4 GHZ ISM BAND

Andrew H. Kemp — Edmund B. Bryant *

A 2.45 GHz pulse compression, channel impulse response (CIR) system is described. The motivation for its development and results verifying its performance are given. The system is shown to be an effective test and measurement tool for analysis of 2.4 GHz ISM band channels particularly for spread spectrum communication system deployment. The required signal processing is described and, because of the importance of spurious free dynamic range, the potential effects of even small inter-modulation products are considered.

K e y w o r d s: channel sounder, channel impulse response, delay spread, spread spectrum

1 INTRODUCTION

In project MOFDI [1], a spread spectrum system is being developed to provide wireless communications for industrial control applications. Primarily because of its worldwide availability the 2.4–2.483 GHz ISM band has been selected for MOFDI. For this reason and its unlicensed nature many other communications systems have targeted this band such as IEEE802.11 wireless LANs and Bluetooth PANs. In the MOFDI application interference from these other systems can be mitigated by excluding such devices from the industrial sites in question. The system described here will measure the extent to which the propagation environment will cause communications systems to 'self-interfere' (*ie* suffer from inter-symbol interference, ISI) as a result of multi-path propagation. Although this system is developed specifically for the MOFDI purpose it is also applicable to investigate the level of multi-path propagation which can be expected for other systems operating in the 2.4 GHz ISM band.

The MOFDI system will be required to operate in a wide range of industrial environments including chemical process plants, electricity transformer stations, mines and manufacturing plants. Characterisation of this range of environments at 2.4 GHz has not previously been reported and the details of the channel impulse response measurement system developed for this is reported here. It is noteworthy that reports of measurements in similar (though not identical) environments and at lower frequencies stress the need for environment-specific and frequency-specific measurements [2], [3]. The characteristic statistics of these environments (predominantly the root mean squared (RMS) delay spread is used [4]) are calculated from the power delay profile. This equipment measures the power delay profile. The 'normalised RMS delay spread' is calculated by dividing the RMS delay spread by the symbol period. For example a channel with an RMS delay spread of 100 ns and a symbol rate of 1 MSymbols per second would have a normalised RMS delay spread of a tenth. A useful rule-of-thumb in determining the impact of dispersion on the reliability of a communications system, without an equaliser, is that a bit error ratio (BER) of greater than 10^{-3} would be expected if the normalised RMS delay spread is greater than a tenth.

Following this introduction, section 2 of this paper describes the pulse compression method that the system is based on. Next, in section 3, the developed system is detailed. In section 4 the signal processing of the recovered waveform is described. Results, which verify the performance, are then discussed in section 5 prior to finally concluding the paper.

2 MATHEMATICAL BASIS OF TECHNIQUE

In measuring the impulse response of a linear system the problems associated with exciting the system with a high amplitude, short duration signal, *ie* an impulse, may be avoided by using a pseudo-noise (pn) signal for excitation and crosscorrelating the input and the output [5].

$$\phi_{ny}(k) = \phi_{nn}(k) * h(k)\,. \tag{1}$$

Where ϕ_{ny} denotes crosscorrelation and ϕ_{nn} denotes autocorrelation, $h(k)$ is the impulse response of the system under test. Additionally, by using the crosscorrelation of a reference pn signal with the output pn signal once it has been distorted by the system under test, allows the suppression of noise which can be expected to have a random contribution over the period of the test. The disadvantage of this noise suppression method is the extension of the test period which reduces the temporal resolution

* Institute of Integrated Information Systems, School of Electronic and Electrical Engineering, University of Leeds, LS2 9JT UK
Email: A.H.Kemp@ee.leeds.ac.uk

ISSN 1335-3632

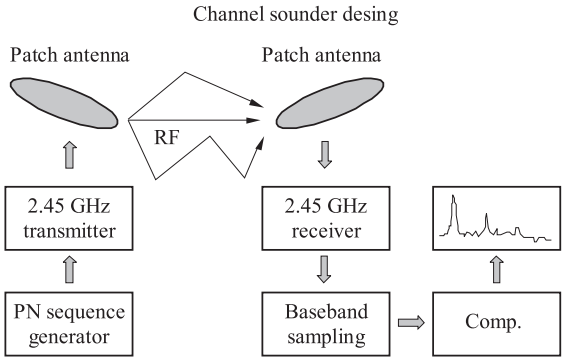

Fig. 1. Block diagram of the CIR system

of the measurement. This is detrimental to the ability to measure Doppler effects resulting from variations in the propagation channel and environment during the period of the test.

The pn sequence used in a pulse compression system is required to have an 'impulsive' auto-correlation function, *ie* one with zero side lobes and non-zero in-phase correlation. The well known maximal-length sequences (or m-sequences) have such properties [6] and the selection of which particular m-sequence depends on the sequence length required and the terms of the generator polynomial. The sequence length will determine the 'coding gain' provided by the sequence, *ie* the ability of the sequence to provide a signal-to-noise gain through time spreading of the signal energy during transmission. The nature of the generator polynomial determines the characteristics of the sequence generated, *ie* maximum-length or non-maximum length. The density of the primitive polynomial defining the sequence, *ie* the number of terms in the polynomial, determines the order of the binary digit strings.

This system uses a 511-chip m-sequence to provide a coding gain of 54 dB. The irreducible polynomial has three terms and corresponds to a cycle length of $511 = 2^9 - 1$ [7]. The particular m-sequence chosen is described by the irreducible polynomial [7]:

$$f(x) = X^9 + X^4 + 1\,. \tag{2}$$

This Boolean sequence is mapped to the binary input signal by arbitrarily mapping the logic 0 values to negative voltages and the logic 1 values to positive voltages. A pulse shaped version of the sequence is the actual input to the transmission system (as discussed in section 3.1.The impulse response of the channel under test convolved with the auto-correlation function of the sequence results in the crosscorrelation of the input and the output (as given in equation (1)). Since the periodic auto-correlation of an m-sequence is an approximate delta function,

$$\phi_{nn}(k) \approx \delta(k)\,, \tag{3}$$

the result of convolving any function with it, is the function itself. Hence, convolving the periodic auto-correlation function of the m-sequence with the impulse response, results in the impulse response of the system under test. Consequently, the impulse response of the channel under test, can be derived by crosscorrelating the noise-like input (the m-sequence) with the output (*ie* the received signal, which is the m-sequence distorted by the channel). It should be noted that the desirable, impulsive auto-correlation function of m-sequences only occurs when they are treated periodically. In the system described here the software processing of the received signal takes a 'sliding correlation' of succeeding 511 chip sections of the incoming waveform, with the m-sequence, to calculate the periodic crosscorrelation and hence derive the channel-under-test impulse response.

The m-sequence is generated at a rate of 25 Mchips per second (where a 'chip' is a binary digit or element, of the sequence); hence, the 511 chip sequence repeats every $20.44\,\mu$s. Consequently the maximum Doppler frequency this sequence can resolve is 24.461 kHz. Recordings last for 5 ms, providing a minimum Doppler resolution of 200 Hz. Also, for maximum noise suppression (at the expense of resolving Doppler-shifted components) averaging can be taken over 244 cycles of the sequence. This gives a factor of $\sqrt{244} = 15.6$ improvement in signal to noise ratio.

3 TEST SYSTEM DESCRIPTION

Subsections 3.1 and 3.2 below detail the transmitter and receiver elements of the test system. A separate section details the antennas used (section 3.3). One of the design aims of this realisation was to use 'off-the-shelf' components where possible, since there is little point in doing unnecessary design work, particularly for a one-off solution. In the transmitter section of the system it was initially hoped to be able to obtain an off-the-shelf signal generator, but a device fast enough (*ie* at 100 MSamples per second) for this application, and not excessively cumbersome or 'power hungry', was not available. So for this section a specific solution was designed and implemented.

At the receiver, subsequent to RF down-conversion and demodulation, a fast oscilloscope is used to provide the digital sampling of the incoming analogue waveform and the processing is then performed on a digital computer (a laptop PC). The data is transferred from the oscilloscope to the PC via the general purpose interface bus (GPIB). The test system block diagram is shown in Fig. 1.

3.1 Transmitter

The transmitter comprises a signal generator, which generates the pulse shaped samples of the m-sequence (this is detailed in sub-section 3.1.1), and the RF section which mixes the smoothed pulse sequence up to the channel under test (and is detailed in sub-section 3.1.2). The

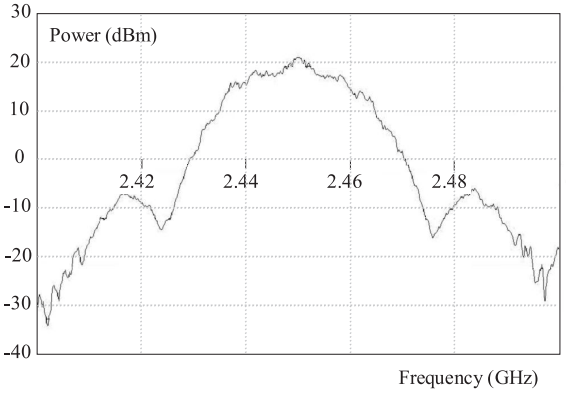

Fig. 2. The spectrum of the transmitted, pulse shaped pseudo-noise sequence.

whole transmitter, excluding the antenna but including rechargeable battery power source, is housed in a robust flame and water -proof 'peli-case' to aid it's deployment in potentially hazardous industrial environments.

3.1.1 Signal generator

The transmitted signal is a pulse shaped, 511-chip m-sequence (see section 2). The frequency spectrum of a 511-bit m-sequence has a $sin(x)/x$ shaped envelope with first nulls at $\pm 2 f_H$. This frequency is generated by the fundamental frequency of a binary '1' followed by a binary '0' in the sequence *ie* $f_H = 1/(2 * period_{chip})$. $f_H = 12.5$ MHz for a chip period of 40 ns. The spectral lines within this $sin(x)/x$ envelope are separated by the lowest frequency component in the sequence, f_L, which is a result of the period of the whole sequence. $f_L = 1/(511 * period_{chip}) = 48.924$ kHz. This wideband signal source is used to measure the impulse response over the bandwidth of ±12.5 MHz about the carrier frequency, *ie* a −3 dB bandwidth of 25 MHz in total. However, it is necessary to pulse-shape the sampled sequence to suppress the spectral components outside the first nulls (±25 MHz). This is to prevent them from causing out-of-band radiation and in-band inter-modulation noise. Communications systems typically use raised cosine pulse shaping to minimize out-of-band radiation but this relies on knowledge of the sample instant. In the measurement system described here, the multi-path components of the impulse response will inevitably occur at unspecified instants so Gaussian pulse shaping was selected. Gaussian pulse shaping does not require knowledge of the sample instant. A five tap digital filter provides this pulse shaping, with −3 dB point at 17.5 MHz. The RF spectrum of the transmitted sequence can be seen in Fig. 2.

The methodology described in the previous chapter is used to generate a sequence of 8-bit samples which are cyclically output from a block of memory at 100 MSamples per second. There are four samples output per pulse shaped, m-sequence chip, thereby exceeding the Nyquist criterion of greater than two samples per period. The output from the signal generator forms the input to the RF section of the transmitter.

3.1.2 Transmitter RF section

The transmitter RF section is a three stage design (see Fig. 3) with intermediate frequencies (IFs) of 130 MHz and 600 MHz prior to an RF output at 2.45 GHz. Phase stability between the transmitter and receiver is maintained by the use of temperature stabilised 10 MHz crystal oscillators at the transmitter and receiver; all local oscillator frequency sources are synthesised using these sources as references. The stability of the 10 MHz reference is chosen so that the cycle frequency of the m-sequence (48.924 kHz) will be at least 10 times greater than the maximum baseband frequency offset due to oscillator drift in the non-coherent system. This will minimise the effect that phase rotation will have on the correlation process. For this system, the reference oscillator stability is better than ±0.01 ppm over a −20 °C to +70 °C temperature range, ±0.00005 ppm short term, and ±0.1 ppm per year due to ageing. This equates to a guaranteed maximum frequency offset of $2450 * 0.2 = 490$ Hz at baseband over the period of a year, well within the specified limit of 4.9 kHz.

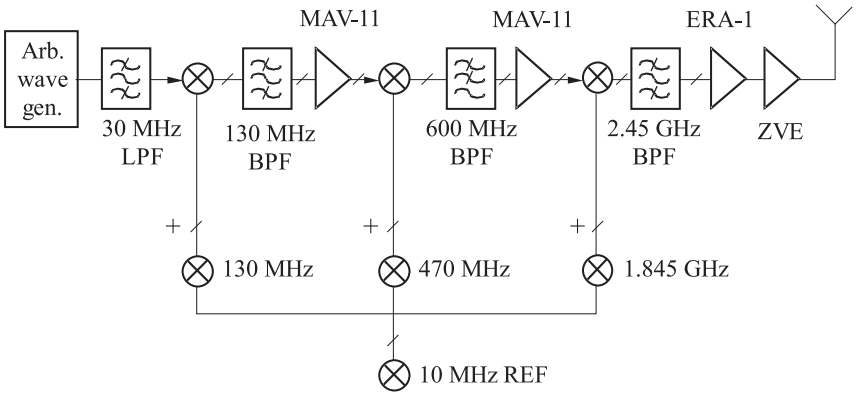

Fig. 3. Schematic diagram of the transmitter

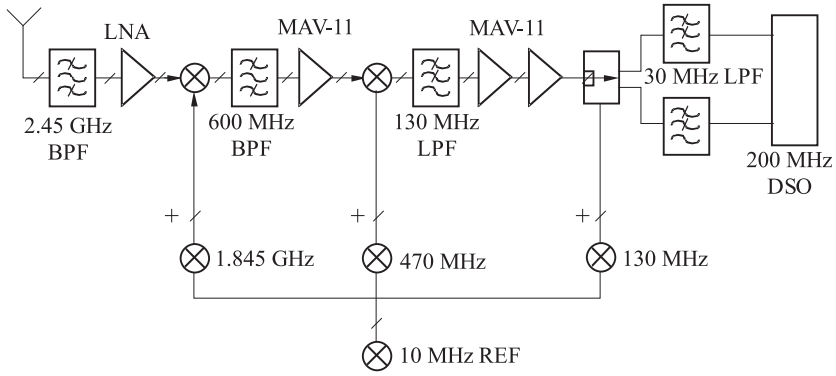

Fig. 4. Schematic diagram of the receiver

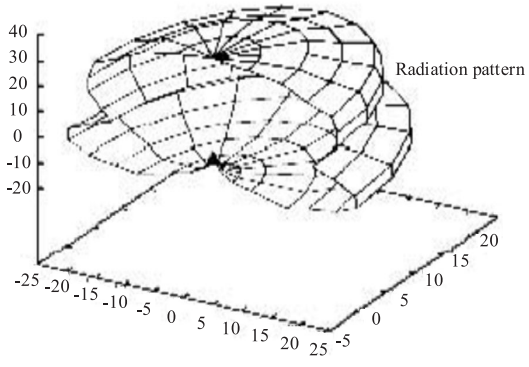

Fig. 5. The measured radiation pattern of the TM_{01} antenna

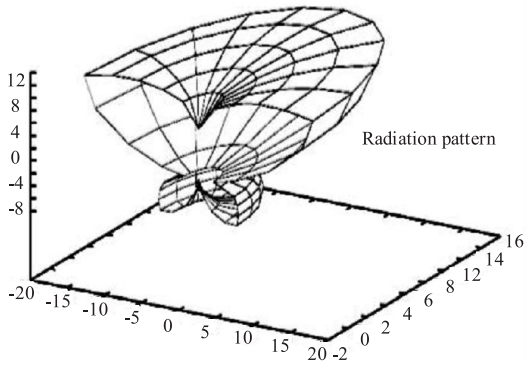

Fig. 6. The measured radiation pattern of the TM_{02} antenna

Peak output power of the system (at 1 dB compression) is 27 dBm. However the wideband nature of the transmitted waveform reduces the compression point to 23 dBm. The waveform amplitude can be adjusted in the signal generator to optimise system performance. In-band harmonics from poor system design or amplifier/mixer compression and poor group-delay responses in filters will cause false correlation peaks in the processed received waveform, thus corrupting the CIR measurements. Because of the required spurious-free dynamic range of the processed output (30 dB), even small harmonics must be avoided. It is therefore imperative that the system is designed to avoid input levels being brought close to compression points. Because of this, all components must be specified to provide reliable system operation, with most emphasis on the final power amplifier.

3.2 Receiver

The receiver is larger than the transmitter since it includes three units: the RF down-converter, a sampling oscilloscope and a laptop PC. Consequently, during measurements, the transmitter is placed in the least accessible end of the measurement link and the receiver typically operated from a trolley. Power for this section of the system is supplied from either a battery or a mains supply. The following subsection describes the structure of the receiver and is followed by a description of the RF section of the system. Section 4 is dedicated to describing the signal processing which takes place in the PC. The signal processing recovers the power delay profile (pdp) from the received signal, uses averaging to suppress the noise, and calculates the statistics of the delay spread.

3.2.1 Receiving system structure

The received signal waveform is initially down-converted and demodulated by the RF section (which is described in section 3.2.2, below). The de-modulated, baseband waveform is then digitised by the input stage of an HP54645B digital storage oscilloscope. It is capable of simultaneously sampling 5 ms of data from both in-phase and quadrature (I and Q) channels at 200 MSamples per second. Each sample is of 8 bit resolution which provides ± 128 digital voltage quantisation levels, giving 42 dB of dynamic power range.

The recording of the waveform is controlled from a PC via the GPIB and the data is subsequently downloaded to the PC, again via the GPIB. Each 5 ms recording comprises of 2 Mbytes of data and takes of the order of 10 seconds to download before re-sampling can occur.

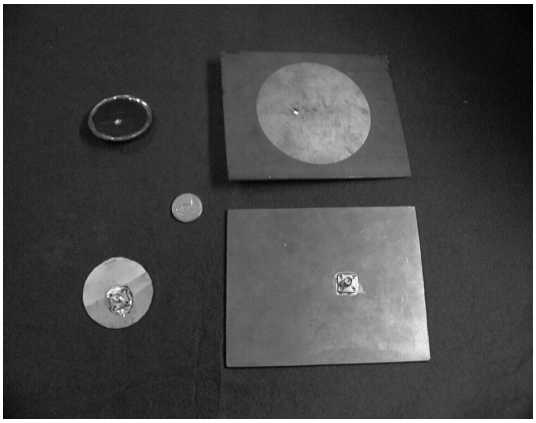

Fig. 7. A picture of the TM_{01} antenna (on the left) and TM_{02} antenna (on the right)

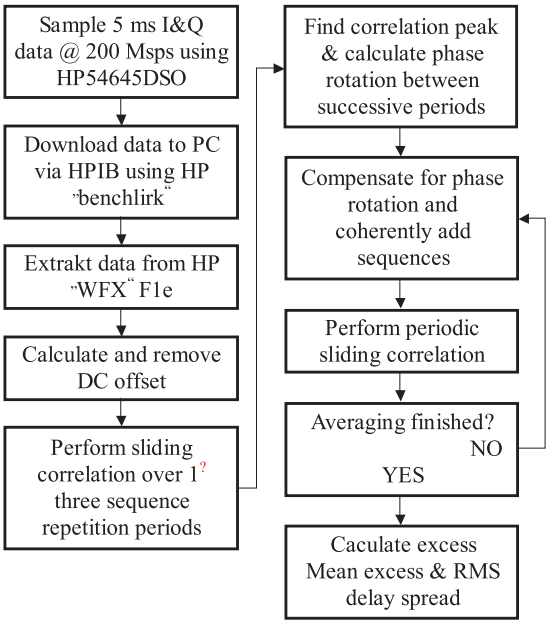

Fig. 8. Flow diagram of signal processing performed on the baseband received signal.

The constituent elements of the CIR measurement system are shown in Fig. 1.

3.2.2 Receiver RF section

The RF section of the receiver is of a similar structure to the transmitter with the replacement of the baseband mixer by a quadrature demodulator (see Fig. 4). Again a three-stage architecture is employed with the same IFs. The noise floor of the receiver has been measured to be −93.2 dBm, and the dynamic range (noise floor to the 1 dB compression point) for a sinusoidal input is 53.5 dB, dropping to 49.5 dB for a wideband input. However, this is not a usable dynamic range for CIR measurements because of the tight impulse response spurious free dynamic range (IRSFDR) requirements; it is approximately 45 dB in this practice.

3.3 Antennas used

To date, measurements made with the CIR, have used two circular patch antennas, a TM_{01} mode and a TM_{02} mode antenna, and dipole antennas, all matched to 50 Ω at 2.45 GHz. The radiation patterns of the two patch antennas, which are omni-directional in azimuth, are given in Fig. 5 and Fig. 6; also an illustration of the practical implementation of the two patch antennas is shown in figure Fig. 7. The TM_{01} mode patch antenna has the main lobe directed in the normal direction whereas the TM_{02} mode antenna has its main lobe at $\pi/2$ to the normal and a null in the normal direction [9]. These two, simply implemented antenna designs, were selected, not only for their radiation patterns (as explained below) but also because they can be cheaply and robustly implemented for the sometimes hostile environments of industrial plants. In particular, the TM_{02} mode antenna with its overhead null (when mounted horizontally) was considered a practical solution in locations where either sky or a reflector was above the antenna. Both these environments could result in wasted transmit power since either power will be transmitted into space or reflected back to the transmitter. The TM_{02} antenna, will not waste power in the overhead direction but will radiate omni-directionally at 45° to the horizontal. This will maximise transmission via reflections from adjacent surfaces which is considered of particular importance in the industrial environment, especially where triple base station diversity may be used to achieve the required bit error ratio (BER) [10]. Conversely the TM_{01} mode antenna has a main lobe in the normal direction. Conceptually it was considered that the lobe could be successfully 'pointed' in the direction deemed necessary for transmission. Measurements were taken using both antennas in a wide range of environments to investigate these hypotheses. That ongoing work will be reported separately.

4 SIGNAL PROCESSING OF RECEIVED SIGNAL

The sampled measurement data is processed off-line, this being possible immediately after sample download for measurement validation. A flow diagram of the signal processing operation is shown in Fig. 8. Data processing software was developed specifically for the system and it provides the following features:

- Initially the data-file, which exists in a proprietary Hewlett Packard binary format, is parsed to remove header information and obtain instrument settings. During this parsing , the I- and Q- channel DC offsets of the data are calculated so that such offsets can be removed (this is most important for small scale settings from long range measurements or high attenuation paths).

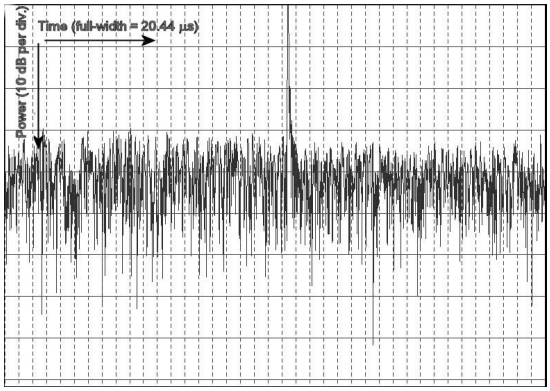

Fig. 9. Output from the signal processing software for an unaveraged data set

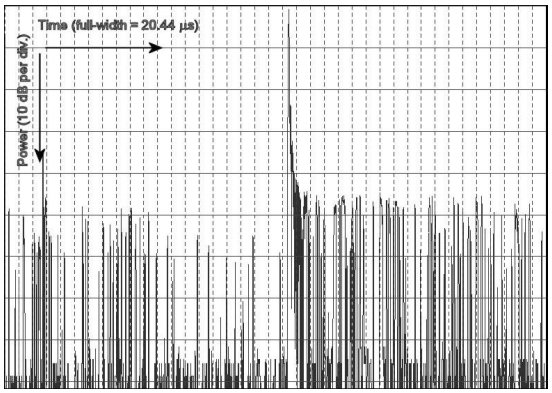

Fig. 10. Output from the signal processing software for averaged data set

- Data is correlated as a continuous set with the original m-sequence sliding at 5 ns intervals, with 1 chip interval between contiguous sequence samples. This provides an 8 times over-sampled correlation output.
- Phase rotation due to reference oscillator drift in the transmitter and receiver is compensated for linearly on a sequence-by-sequence basis to provide a coherent set of impulse responses. This is not so important for single sequence correlation because of the inherent stability of the temperature-controlled references. However, any averaging of an uncompensated dataset would become increasingly unreliable with the averaging size due to phase cancellation effects. Averaging of the data can be user defined between 0–244 averages; this upper limit is imposed by the maximum duration of a record.

Any sequence timing offset due to the instability of clocks in the sampling oscilloscope and sequence generator can also be compensated for; again this is more important as the number of averages increases.

The graphical representation of the impulse response is updated on an average-by-average basis, allowing the confirmation of the compensation procedures. When this process is finished, the full $20.44\,\mu$s correlation result is displayed. A $2\,\mu$s window of the impulse response can then be displayed with the corresponding excess delay, mean excess delay (MED) and RMS delay spread (RDS) results. All results are calculated from the leading edge of the first peak crossing the -30 dB threshold (relative to the peak's maximum value), with the trailing edge of the last crossing being utilised for calculation of the MED and RDS.

Figures 9 and 10 illustrate examples of the final output of the signal processing software. These figures are for an un-averaged and an averaged dataset respectively from a coaxial link between the transmitter and receiver. The IRSFDR of the system can be seen to be 30 dB for the unaveraged and 40 dB for the averaged dataset. The slight hump in the main lobe is caused by non-linearitys in the baseband mixer stage. It does not affect the RDS results significantly.

5 VERIFICATION MEASUREMENTS

The purpose of this CIR measurement system is primarily to allow the gathering and validation of the results from a propagation simulation tool for predicting the propagation characteristic in previously uncharacterised industrial environments. The output from the propagation simulator tool will be used to assess the propagation in the industrial sites and, from this, to optimally locate base stations for a cellular communications system. However, prior to this validation of the propagation simulator through use of the CIR measurement system, it is first necessary to verify that results from the CIR are correct. This verification is done by measuring the CIR of a known environment and examining the result to confirm that it is as expected.

5.1 Test procedure

For reasons of convenience, a test range in an adjacent park area has been used for the verification measurements. This test range includes:

- a mausoleum, which provides the main signal reflector,
- a $0.56\,\mathrm{m}^2$ sheet of aluminium used as a temporary reflector,
- tall buildings surrounding the park area (ranging from four to six stories) and
- numerous trees.

The diagram in Fig. 11 shows the test set-up. The transmitter and receiver were separated by approximately 24 m and using TM_{01} mode directional antennas (see section 3.3) with the main lobe directed toward a point on the mausoleum wall midway between them. Additionally the temporary reflector, the sheet of aluminium, was placed in position marked R_T. Measurements were taken initially without the temporary reflector, and subsequently with it in position R_T.

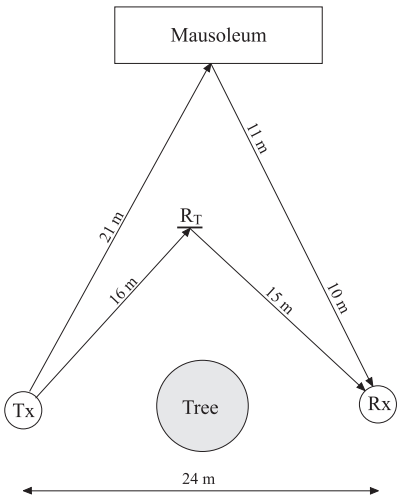

Fig. 11. The experimental set-up used for the verification measurments

5.2 Results obtained

The first 500 ns of the power delay profile (pdp) recovered from both the measurements described above is shown in Fig. 12. These profiles illustrate the complex spread of received signal, even in the simple test environment chosen. The first arrival of both pdps is due to the line-of-sight (LOS) propagation directly from the transmitter to the receiver. A tree existed on this path but this simply serves to reduce the amplitude of the first arrival relative to the subsequent paths. The subsequent peaks are attributable to reflections from the mausoleum and the temporary reflector as follows. The LOS path length is $\sim 24m$ and the path including a single reflection at the mausoleum is of length $\sim 42m$; hence the propagation reflecting from the mausoleum will arrive $\sim (42-24)/3*10^8$ seconds after the LOS path arrival, *ie* ~ 60 ns. Similar analysis of the path reflecting from the temporary reflector at location R_T gives relative delay after the LOS arrival of ~ 23 ns. However, the chip period of the system (as described in section 3.1.1) is 40 ns. Consequently differences in path length of less than 12 m will not be discernable. Since the difference in path length for R_T is ~ 11 m, it is not separately discernable but its presence disperses the signal arriving from the LOS path and the path with the single reflection from the Mausoleum. This is confirmed by examination of Fig 12.

5.3 SAMPLE RESULTS FROM AN INDUSTRIAL SITE

Preliminary testing with the system described, has taken place on a range of industrial sites and an example of the output from the equipment is given here. The particular measurement shown below in Fig. 13 is the result of making a channel impulse response measurement on the BP-Amoco site at Wytch Farm, UK. This plant is a Petroleum Gathering Station and contains a large amount of metallic pipe structure. An illustration of the site is provided in Fig. 14. The RMS delay spread calculated for this power delay profile is 80 ns. A full discussion of results obtained on a number of industrial sites is currently being prepared for publication.

6 CONCLUSIONS

This paper has described a CIR measuring system for the 2.4 GHz ISM band. This CIR system is currently being used to investigate propagation characteristics experienced by spread spectrum communications systems

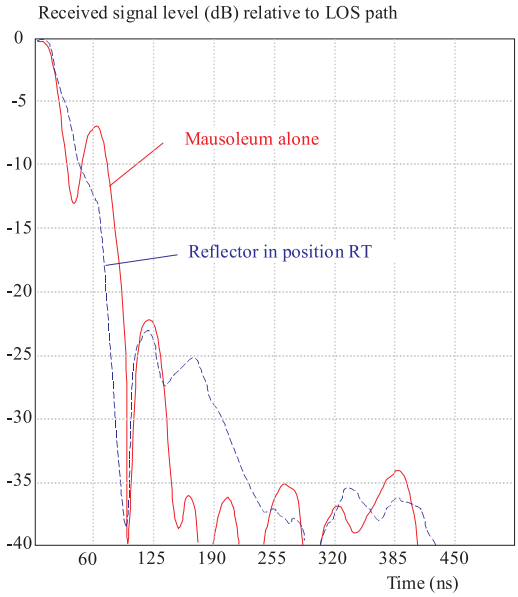

Fig. 12. Power delay profile measured in park area for verification of CIR systems

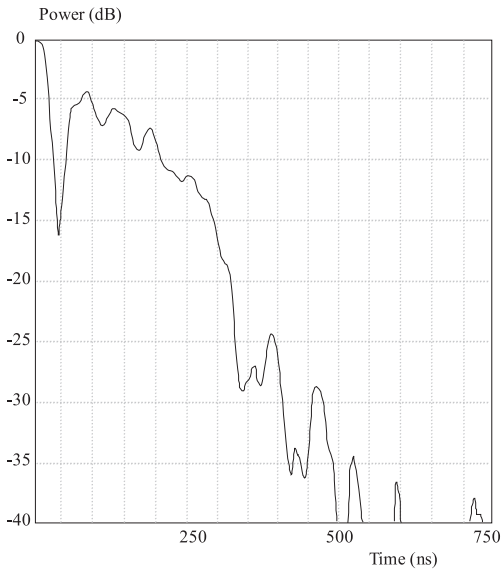

Fig. 13. Preliminary power delay profile from BP-Amoco Petroleum gathering station

using this band. The paper demonstrates the measurement system gives more than 30 dB of received signal-to-noise ratio and that it has low system noise. The post-measurement signal processing and noise suppression, which is performed on the received signal waveform, allows signal averaging to further reduce the noise level, giving a signal-to-noise ratio of greater than 40 dB. At the transmitter, digital filtering of the pn pulse sequence (the Gaussian pulse shaping) band limits the signal to ±17.5 MHz. The receiver eight-times over-samples the received waveform. This received signal is band-limited by the 40 MHz bandwidth of the intermediate frequency stage of the receiver, making it possible to resolve the multipath components separated by less than the 40 ns chip period. Section 5 establishes the accuracy of the channel measurement system, particularly when providing information to support spread spectrum communication systems operating in the 2.4 GHz ISM band.

Fig. 14. Preliminary power delay profile from BP-Amoco Petroleum gathering station

Acknowledgement

This work has been funded by the Engineering and Physical Sciences Research Council (EPSRC) of the UK.

References

[1] MOFDI an EC framework 4 (FP4) project with the reference number ESPRIT 27035..

[2] ESPINOSA, J.—MONTERO, M.—HERNANDO, J. M.—PÉREZ, F.—MILANÉS, J. A.—HIDALGO, I.—GALLARDO, M.: Coverage Simulator for Wireless Networks, IEEE International Workshop on Factory Communications Systems, WPCS Proceedings, Universidad Politecnica de Madrid, Madrid, Spain, 1997, pp. 149–156.

[3] RAPPAPORT, T.—SEIDEL, S. Y.—TAKAMIZAWA, K.,: Statistical Channel Impulse Response Models for Factory and Open Plan Building Radio Communication System Design, IEEE Transactions on Communications **39** No. 5 (1991), 794–807.

[4] ANDERSON, J. B.—RAPPAPORT, T. S.—YOSHIDA, S.: Propagation Measurements and Models for Wireless Communications Channels, IEEE Communications Magazine (January 1995), 42–49.

[5] BORISH, J.—ANGELL, B.: An Efficient Algorithm for Measuring the Impulse Response Using Pseudorandom Noise, Journal of the Audio Engineering Society **31** No. 7 (1983), 478–488.

[6] MUTAGI, R. N.: Pseudo Noise Sequences for Engineers, IEE Electronics and Communications Engineering (April 1996).

[7] SCHNEIER, B.: Applied Cryptography, 2 edition, Wiley, 1996.

[8] FAN, P.—DARNELL, M.: Sequence Design for Communications Applications, 1 edition, Research Studies Press, 1996.

[9] GUO, Y. J.—PAEZ, A.—SADEGHZADEH, R. A.—BARTON, S. K.: A Circular Patch Antenna for Radio LAN's, IEEE Transactions on antennas and propagation **45** No. 1 (January 1997), 177–178.

[10] KEMP, A. H.—PHILIPS, A.—ORRISS, J.—BARTON, S. K.: High Inegrity Wireless Communications over a Channel Exhibiting Severe Multi-Path Propagation, VTC 1999-Fall, Gateway to 21st Centuary Communicaitons Village, VTC Proceedings, Amsterdam, September 1999.

Received 25 October 2005

Andrew H. Kemp (Dr) was born in Portsmouth, UK in 1963. After a state education he graduated from the University of York with a BSc in Electronics in 1984. After time in industry he returned to academia at the University of Hull in 1987 and under the direction of Professor Darnell achieved a PhD in 1991 entitled 'Complementary sequences and their use in multi-functional communications system architectures'. He again spent time in industry prior doing post-doc work at the University of Bradford before moving to the University of Leeds where he is currently lecturing. His primary research interests are in multipath propagation and quality of service issues for wireless Internet traffic.

Edmund B. Bryant (Dr) was born in Staffordshire, UK in 1967. After a state education he graduated from Leeds Polytechnic with a BEng in Communication Engineering in 1990. He received a NERC case award for a doctorate at the University of Sheffield in 1991, and achieved a PhD in 1995 entitled 'Radio Tracking of Pinnipeds'. He was subsequently employed by the NERC Sea Mammal Research Unit as a Research Fellow investigating low power radio location systems. In 1997 he spent time in industry designing electronic warfare receivers until he returned to academia at the University of Leeds in 1998. His primary research interests were in channel sounder design and multipath radiowave propagation studies. He left the University of Leeds as a Senior Research Fellow in 2003 to run his own company developing GPS receivers for marine animal research.